PHYSICAL REVIEW D VOLUME 52, NUMBER 4 15 AUGUST 1995

Quantum electrodynamics at large distances. II. Nature of the dominant singularities

Takahiro Kawai
Research Institute for Mathematical Sciences, Kyoto University, Kyoto 606-01, Japan

Henry P. Stapp
Lawrence Berkeley Laboratory, University of California, Berkeley, California 94720
(Received 22 September 1994)

Accurate calculations of macroscopic and mesoscopic properties in quantum electrodynamics require careful treatment of infrared divergences: Standard treatments introduce spurious large-distances effects. A method for computing these properties was developed in paper I. That method depends upon a result obtained here about the nature of the singularities that produce the dominant large-distance behavior. If all particles in quantum field theory have a nonzero mass then the Landau-Nakanishi diagrams give strong conditions on the singularities of the scattering functions. These conditions are severely weakened in quantum electrodynamics by the effects of points where photon momenta vanish. A new kind of Landau-Nakanishi diagram is developed here. It is geared specifically to the pole-decomposition functions that dominate the macroscopic behavior in quantum electrodynamics, and leads to strong results for these functions at points where photon momenta vanish.

PACS number(s): 12.20.Ds, 11.15.Tk, 11.55.Bq

I. INTRODUCTION

A method of calculating the macroscopic and mesoscopic properties of scattering functions in quantum electrodynamics was developed in Ref. [1], in the context of a particular example. The large-distance behavior was shown to be concordant with the idea that electrons propagate over large distance like stable particles in classical physics. This result is expected, and indeed is required in the interpretation of scattering experiments. But unless one is able to *deduce* this dominant behavior from the theory, and exhibit a controlled nondominant remainder, the theory would be unsatisfactory, for it would lack the power to make valid predictions in the mesoscopic regime lying between the quantum and classical realms. This regime is becoming increasingly important for technology.

The extraction from quantum electrodynamics of the correspondence-principle large-distance part plus a well-controlled nondominant remainder is a not a trivial exercise. Difficulties arise from (1) the spurious large-distance effects introduced by the usual momentum-space treatments of infrared divergences, (2) the singular character of the photon-propagator singularity surface $k^2 = 0$ at $k = 0$, (3) the occurrence of several different types of singularities on certain singularity surfaces, and (4) the need to deal effectively with the pole-decomposition functions that control the large-distance properties. These problems were all dealt with in Ref. [1]. But one key property was left unproved. The immediate aim of this paper is to establish this property. In the course of doing so we shall develop powerful methods for dealing with singularities arising in quantum electrodynamics.

A first problem to be faced is the weakening of the Landau-Nakanishi diagrammatic conditions for the presence of a singularity. The vanishing of the gradient of k^2 at $k = 0$ renders the original versions [3,4] of these conditions trivial: They yield no condition at all, for functions that describe processes with internal photons. Improved versions that cover the $k = 0$ points have been devised [5]. But these also have too many solutions: In general a *continuum* of essentially different diagrams all lead to any given point on the Landau singularity surface. This surplus of diagrams precludes the application of the simple known rule [6] for the nature of the singularity on that surface.

The first part of our resolution of the problem is this: Use not the original momentum-space variables, but rather a set of nested radial coordinates and the associated angles. These variables are defined by first separating the integration region into sectors specified by the different orderings of the relative sizes of the Euclidean norms $|k_i|$ of the soft-photon energy-momenta k_i, then, in each sector, reordering the vectors k_i by size, so that $|k_i| \geq |k_{i+1}|$, and finally writing

$$k_i = r_1 r_2 \cdots r_i \Omega_i \ , \tag{1}$$

where, for all i, $|\Omega_i| = 1$ and $0 \leq r_i \leq 1$.

A second problem is that we need results not for the scattering functions themselves but rather for the functions obtained from them by decomposing their meromorphic parts into sums of poles times residues. The functions obtained by this pole decomposition give the dominant large-distance behavior. We devise a new kind of "Landau" diagram for these functions.

The specific example considered in Ref. [1] pertains to a Feynman graph consisting of six hard photons coupled to six vertices into a single charged-particle closed loop.

These six vertices are divided into three disjoint pairs, with the two vertices in each pair linked by a charged-particle line that is associated with a momentum-energy vector that is far off mass shell. This line can, for our purposes, be shrunk to a point. This produces a (triangle) graph G consisting of three internal charged-particle lines, with two hard photons attached at each of the three vertices.

We now "dress" this triangle graph G with soft photons: We consider the set of graphs $\{g\}$ obtained by coupling all possible numbers of soft photons into this charged-particle loop in all possible ways. If we separate the interaction term $ie\gamma_\mu$ into its classical and quantum parts, in the way described in Ref. [1], then all the classical interactions can be shifted to the three hard vertices, leaving only quantum vertices along the three sides of the triangle. Each of these three sides s of the original triangle graph G is therefore now divided into segments by a set of quantum vertices. Each segment j is associated with a Feynman denominator $(p_s+K_j)^2-m^2+i0$, where K_j is some (algebraic) sum of photon momenta. The total contribution from all "classical photons," which are the photons that are coupled into G *only* at classical vertices, can be factored off as a single unitary operator that is independent of the nonclassical remainder.

We are interested here in the properties of the individual terms of the perturbation expansion of this remainder. Each such term is represented by a Feynman graph g. Each soft photon is coupled on one or both ends into either a vertex or a side of the original triangle graph G, with C couplings at vertices and Q couplings on the sides.

To exhibit what are expected to be (and turn out to be) the dominant contributions to the singularity of the scattering function on the triangle-diagram singularity surface $\varphi=0$, we consider the Feynman denominator associated with each segments j of side s to be a pole in the $z_s=p_s^2$ plane, and then express the function associated with each of the three sides s of the triangle as a sum over pole contributions:

$$N_s\prod_{j=0}^{n}[(p_s+K_j)^2-m^2+i0]^{-1}$$

$$=N_s\sum_{i=0}^{n}\{[(p_s+K_i)^2-m^2+i0]D_{si}\}^{-1}\ , \quad (1')$$

where D_{si} is the product over $j\neq i$ of factors $[(p_s+K_j)^2-(p_s+K_i)^2]$.

There is a pole-decomposition formula such as this for each of the three sides s of the triangle. The direct aim of this paper is to show that for each term consisting of photon propagators, together with three factors $f_{s,i(s)}$, one from each side s of G, with $f_{s,i(s)}$ being the $i(s)$th term in the pole-decomposition formula $(1')$ associated with side s, the contours in Ω_i space can be shifted so as to avoid, simultaneously, all singularities in the photon propagators and residue factors. This result plays a crucial role in our arguments. It means, for the case under study, that the part of the scattering function that comes from the meromorphic parts of the propagators can be expressed as a sum of terms, in each of which the only singularities are end-point singularities at $r_i=0$ and $r_i=1$, and three Feynman denominators, one for each of the three sides s of the triangle G. The problems are thereby focused on the effects of the integrals over the r_i. These are the issues resolved in papers I and III.

II. NOTATION

The original triangle graph G is shown in Fig. 1. The momenta p_1, $-p_2$, and p_3 represent the momenta flowing from v_2 to v_1, from v_2 to v_3, and from v_1 to v_3, respectively. Conservation of energy-momentum is represented by introducing a closed loop carrying momentum p, and two open paths carrying momenta q_1 and q_3, respectively, in the directions indicated by the arrows. Then $p_1=p+q_1$, $p_2=p-q_3$, and $p_3=p$.

The function associated with this Feynman graph G has a singularity on the positive-α Landau-Nakanishi triangle-diagram singularity surface $\varphi(q)=0$, where $q=(q_1,q_2,q_3)$ and $q_3\equiv-q_1-q_2$. For each point q on this surface $\varphi=0$ there is [2] a uniquely defined set of three four-vectors $p_1(q)$, $p_2(q)$, and $p_3(q)$ such that the singularity at q of the Feynman function $F(G)$ corresponding to the graph G of Fig. 1 arises from an arbitrarily small neighborhood

$$p\approx p(q)=p_1(q)-q_1=p_2(q)+q_3=p_3(q) \quad (2a)$$

in the domain of integration of the Feynman function. These three four-vectors $p_s(q)$ satisfy the mass-shell constraints

$$[p_s(q)]^2=m^2\ , \quad (2b)$$

and the (Landau-Nakanishi) loop equation

$$\alpha_1p_1(q)+\alpha_2p_2(q)+\alpha_3p_3(q)=0\ , \quad (2c)$$

where the α_s are non-negative real numbers. This loop equation implies that for each q on $\varphi(q)=0$ the three four-vectors $p_s(q)$ lie in some two-dimensional subspace of the four-dimensional energy-momentum space.

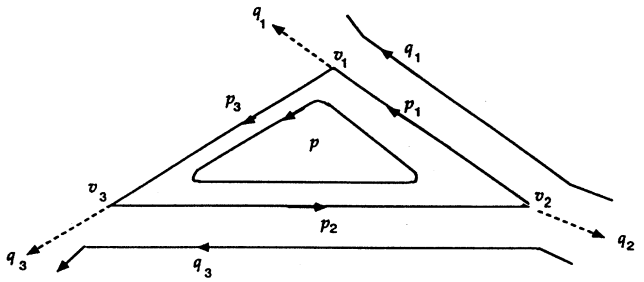

FIG. 1. The basic charged-particle triangle graph G. The momentum-energy p_s flows along side s of the triangle in the direction of the arrow. The three energy components satisfy $p_1^0>0$, $p_2^0<0$, and $p_3^0>0$.

We shall consider a fixed *interior* point q of the surface $\varphi = 0$. In this case each of the three parameters α_s is nonzero, and each of the three four-vectors vectors $p_s(q)$ is nonparallel to each of the other two.

Consider now a graph g obtained by inserting some finite number of soft-photon lines i ($i \in I$) into G. Each inserted line begins on a line of G and ends on a line of G. The bound δ on the Euclidean norms $|k_i|$ of the (soft) photon momenta is taken small enough so that

$$n\delta < \delta' \ll m \ , \tag{3}$$

where n is the number of photon lines in the graph.

The case under consideration here is one where every coupling is a Q-type coupling. For a C-type coupling the corresponding vertex lies on one of the three vertices of the graph G. The present argument can be carried over to the case with some C-type couplings by simply contracting to points some segments representing residue factors, thereby bringing each of various vertices lying on sides of G into coincidence with a vertices of G. These contractions (performed after the loops have been specified) do not upset the arguments.

Momentum-energy conservation is now maintained by introducing a separate closed loop for the momentum k_i of each photon line. Momentum k_i flows along the photon line segment i in the direction indicated by the arrow placed on that line segment. It then continues to flow through the graph g by flowing along certain charged-particle lines of this graph. This continuation through g is specified by the condition that this flow line pass through at most one of the three vertices v_1, v_2, v_3.

The arrow on photon line i is chosen so that every term $p_s k_i$ that occurs in any Feynman denominator occurs with a plus sign. Consequently, the Feynman rule that m^2 represents $m^2 - i0$ is compatible with the rule that each $p_s k_i$ represents $p_s k_i + i0$. No condition is placed on the sign of the energy component k_i^0.

Each charged-particle line segment j has an arrow placed on it. The momentum flowing along the charged-particle segment j in the direction of this arrow is called Σ_j. It is the momentum p_s flowing along the side of the triangle upon which segment j lies, as defined in Fig. 1, plus the (algebraic) sum K_j of the photon momenta k_i carried by the photon loops that pass along this segment j.

Our interest here is in the functions that arise from inserting the pole-decomposition formula (1′) [or (5.5) of Ref. [1]] into the meromorphic parts of the generalized propagators corresponding to the three sides of the original triangle graph G. Consider, for example, the simple graph g of Fig. 2. The meromorphic part of the function represented by the graph g of Fig. 2 is a sum of the four terms represented by the four asterisked graphs of Fig. 3. The asterisk (*) on a line segment of an asterisk graph indicates that it is the segment associated with the (pole) denominator $(p_s + K_i)^2 - m^2 + i0$ in the pole-decomposition formula (1′). Each of the other charge-particle segments $j \neq i$ is associated with a pole-residue denominator function

$$f_j = 2(p_s + K_i)\Omega_{ij} + \rho_{ij}\Omega_{ij}^2 + i0 \ , \tag{4a}$$

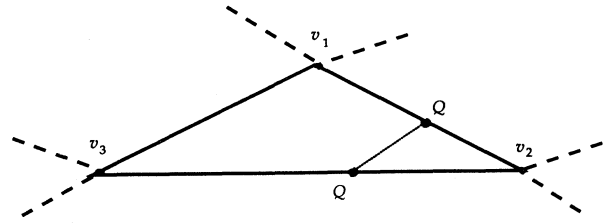

FIG. 2. A graph g representing a soft-photon correction to a hard-photon triangle-diagram process G. Hard and soft photons are represented by dashed and dotted lines, respectively.

where

$$\rho_{ij} = r_1 r_2 \cdots r_{l(i,j)} \tag{4b}$$

and

$$\Omega_{ij} = (\Omega_{l(i,j)} + \cdots) = \sigma_{ij}(K_j - K_i)/\rho_{ij} \ . \tag{4c}$$

The index $l(i,j)$ is the smallest j such that k_j appears in K_i or K_j, but not both. Each of the nonexhibited terms in the parentheses in (4c) is a product of some $\pm\Omega_k$ with a product of a nonempty set of factors r_h ($h \geq 2$).

Each of the pole-residue factors f_j is formed by first taking the difference $\sigma_{ij}(\Sigma_j^2 - \Sigma_i^2)$, where $\Sigma_j = p_s + K_j$ is the momentum energy flowing along segment j in the direction of the arrow on that segment, and $\Sigma_i = p_s + K_i$ is the momentum energy flowing along the asterisked segment on the same side s of the charged-particle triangle, and then dividing out the common factors r_h ($h \geq 1$). The sign σ_{ij} is the sign that makes the term $2p_s k_{l(i,j)}$ in $\sigma_{ij}(\Sigma_j^2 - \Sigma_i^2)$ appear with a positive sign.

The full set of functions f_j whose zeros define the locations of the singularities of the four functions F_g represented by the graphs g of Fig. 3 are given in Table I. The functions f_j for $j = (1, \ldots, 6)$ corresponds to denominators $f_j + i0$. The function f_7 corresponds to the δ-function constraint $\delta(\Omega\tilde{\Omega} - 1)$, and f_8 corresponds to

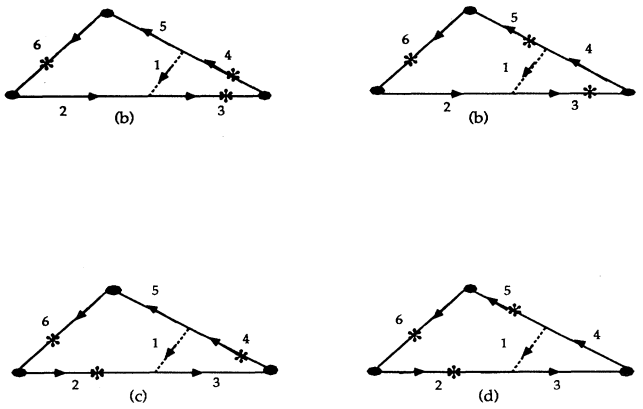

FIG. 3. The asterisked graphs representing the four terms that arise from inserting the pole-decomposition formula (1′) into the meromorphic part of the function represented by the graph g of Fig. 2.

TABLE I. The functions f_j whose zeros define the singularity surfaces of the four functions $F(g)$ represented by the four asterisked graphs of Fig. 3. Here and in what follows p_s, $s \in \{1,2,3\}$, are the vectors defined in Sec. II.

(a)	(b)
$f_1 = \Omega^2$	$f_1 = \Omega^2$
$f_2 = 2p_2\Omega + r\Omega^2$	$f_2 = 2p_2\Omega + r\Omega^2$
$f_3 = (p_2 + r\Omega)^2 - m^2$	$f_3 = (p_2 + r\Omega)^2 - m^2$
$f_4 = (p_1 + r\Omega)^2 - m^2$	$f_4 = 2p_1\Omega + r\Omega^2$
$f_5 = 2p_1\Omega + r\Omega^2$	$f_5 = p_1^2 - m^2$
$f_6 = p_3^2 - m^2$	$f_6 = p_3^2 - m_2$
$f_7 = \Omega\tilde{\Omega} - 1$	$f_7 = \Omega\tilde{\Omega} - 1$
$f_8 = r$	$f_8 = r$
(c)	(d)
$f_1 = \Omega^2$	$f_1 = \Omega^2$
$f_2 = p_2^2 - m^2$	$f_2 = p_2^2 - m^2$
$f_3 = 2p_2\Omega + r\Omega^2$	$f_3 = 2p_2\Omega + r\Omega^2$
$f_4 = (p_1 + r\Omega)^2 - m^2$	$f_4 = 2p_1\Omega + r\Omega^2$
$f_5 = 2p_1\Omega + r\Omega^2$	$f_5 = p_1^2 - m^2$
$f_6 = p_3^2 - m^2$	$f_6 = p_3^2 - m^2$
$f_7 = \Omega\tilde{\Omega} - 1$	$f_7 = \Omega\tilde{\Omega} - 1$
$f_8 = r$	$f_8 = r$

the Heaviside function $\theta(r)$.

The necessary (Landau-Nakanishi) conditions [3,4] for a singularity (in the original real domain of definition) of one of these functions F_g is that there be a set of real numbers $\alpha_1, \ldots, \alpha_8$, not all zero, a real number $r \geq 0$ ($r \leq \delta$), and a pair of real four-vectors Ω and p, with $p_1 = p + q_1$, $p_2 = p - q_3$, and $p_3 = p$, such that

$$\alpha_j f_j = 0 \quad \text{all } j \in \{1, \ldots, 8\} , \tag{5a}$$

and

$$\sum_{i=j}^{8} \alpha_j \frac{\partial f_j}{\partial x_i} = 0 \quad \text{all } i \in \{1,2,3\} , \tag{5b}$$

where $x_1 = \Omega$, $x_2 = r$, $x_3 = p$, and

$$\alpha_j \geq 0, \quad j \in \{1, \ldots, 6\} . \tag{5c}$$

Also,

$$f_7 = 0 \quad \text{and } r \ll m . \tag{5d}$$

The contribution from the upper end points of the r integrals are neglected because these end points are artificially introduced, and hence do not represent singularities of the full function.

The Landau matrix $L_{ij} \equiv \partial f_j / \partial x_i$ for the function represented by the graph of Fig. 3(a) is shown in Table II. The Landau (loop) Eqs. (5b) are formed by multiplying each row j of this matrix by α_j and requiring the sum of each of its columns to vanish.

There are two cases: $r \neq 0$ and $r = 0$. If $r \neq 0$, then Eq. (5a) implies $\alpha_8 = 0$. If one forms the combination of columns $\Omega\, d\Omega - r\, dr$ and compares the entries to Eq. (5a), $\alpha_j f_j = 0$, then one finds that the only term in the resulting loop equations is $\alpha_7 \Omega\tilde{\Omega} = 0$, with $\Omega\tilde{\Omega} = 1$. This entails $\alpha_7 = 0$. If, on the other hand, $r = 0$ then the dr column of L_{ij} has an entry in row 8, and hence it cannot be used in this way. But for $r = 0$, this column does not contribute to $r\, dr$. So in either case the conclusion holds: $\alpha_7 = 0$, and the $\Omega\tilde{\Omega} = 1$ row does not contribute.

Similar arguments in the case of graphs with more lines show that one can always eliminate all of the rows corresponding to $\Omega_i\tilde{\Omega}_i - 1$. In the general case it is the combination of columns $\Omega_i d\Omega_i - r_i dr_i + r_{i+1} dr_{i+1}$ that is used to show the vanishing of the row corresponding to $\Omega_i\tilde{\Omega}_i = 1$. (See Appendix A.)

Consider now the function corresponding to the graph in Fig. 3(d), and the corresponding set of functions f_j in Table I, column (d). This graph is a graph of the separable kind: Cutting the three asterisked segments separates it into three disjoint parts.

If one considers the $d\Omega$ column with the $\Omega\tilde{\Omega} = 1$ row deleted, then one immediately concludes from a look at Table I, column (d), and from the nonparalleled character of $p_2 + r\Omega$, and $p_1 + r\Omega$, and the impossibility of the simultaneous vanishing of f_1 and either f_3 or f_4, that the only solution of the implied Ω loop equation [and Eq. 5(a)] is the trivial one in which all three contributions are zero: $\alpha_1 = \alpha_3 = \alpha_4 = 0$.

In this situation we may invoke a basic lemma [7]: "For any sets of real numbers η_{ba} and λ_{ca} the system of equations

$$\sigma_b = \sum_a \eta_{ba}\delta_a, \quad \sigma_b > 0, \qquad 0 = \sum_a \lambda_{ca}\delta_a , \tag{6a}$$

has a solution $\delta \equiv \{\delta_a\}$ if and only if the system of equa-

TABLE II. The Landau matrix L_{ij} corresponding to the graph in Fig. 3(a). The σ_{js}'s are negative for $j = 2$ and $j = 5$.

f_j	$d\Omega$	dr	dp
$f_1 = \Omega^2$	Ω	0	0
$f_2 = 2p_2\Omega + r\Omega^2$	$p_2 + r\Omega$	$\frac{1}{2}\Omega^2$	Ω
$f_3 = (p_2 + r\Omega)^2 - m^2$	$r(p_2 + r\Omega)$	$(p_2 + r\Omega)\Omega$	$p_2 + r\Omega$
$f_4 = (p_1 + r\Omega)^2 - m^2$	$r(p_1 + r\Omega)$	$(p_1 + r\Omega)\Omega$	$p_1 + r\Omega$
$f_5 = 2p_1\Omega + r\Omega^2$	$p_1 + r\Omega$	$\frac{1}{2}\Omega^2$	Ω
$f_6 = p_3^2 - m^2$	0	0	p_3
$f_7 = \Omega\tilde{\Omega} - 1$	$\tilde{\Omega}$	0	0
$f_8 = r$	0	$\frac{1}{2}$	0

tions

$$\sum_b \alpha_b \eta_{ba} + \sum_c \beta_c \lambda_{ca} = 0, \quad \alpha_b \geq 0, \quad \sum \alpha_b > 0 \qquad (6b)$$

has no solution (α, β)."

Identifying $(\eta_{ba}, \lambda_{ca})$ with the entries in the $d\Omega$ and dr columns of L_{ij}, with $b = j \in \{1, \ldots, 6\}$ and $c = j \in \{7, 8\}$, and identifying $\delta_a = \delta\Omega_a$, for $a \in \{0, 1, 2, 3\}$, as an imaginary displacement of the four-vector contour-of-integration variable Ω, we find from this lemma, and the above-mentioned fact (that the only solution of these equations is the trivial one with every term equal to zero), that at every point in the space of integration variables p and Ω where some set of functions f_j vanishes there is a displacement of the contour in Ω space that shifts the contour away from every Ω-dependent vanishing f_j: By virtue of $(\partial f_j/\partial\Omega)\delta\Omega > 0$ [i.e., (6a)] every such function $f_j(\Omega)$ is shifted by this distortion into its upper-half plane.

We wish to generalize this result. We are particularly interested in the functions represented by separable graphs, i.e., by graphs that separate into three disjoint parts when the three asterisked segments are cut. Another example of such a graph is shown in Fig. 4.

Consider first the case where all $r_i \neq 0$. In this case the Landau equations are equivalent to the Landau equations that arise from using the k-space variables, instead of the (r, Ω) variables. Then the Landau equations associated with the function represented by the graph shown in Fig. 4 can be expressed in a simple geometric form: These equations are equivalent to the existence of a "Landau diagram" (a diagram in four-dimensional space) that has the form shown in Fig. 5. This Landau diagram is a diagram in four-dimensional space (thought of as space-time), and each segment of the diagram represents a four-vector. The rules are as follows.

(1) Each directed photon line segment i represents the vector

$$V_i = \alpha_i k_i \ , \qquad (7a)$$

where k_i is the momentum flowing along segment i of the graph in the direction of the arrow, and $\alpha_i \geq 0$.

(2) Each directed charged-particle segment j corresponding to a pole-residue factor f_j represents the vector

$$V_j = \beta_{js} \Sigma_j \ , \qquad (7b)$$

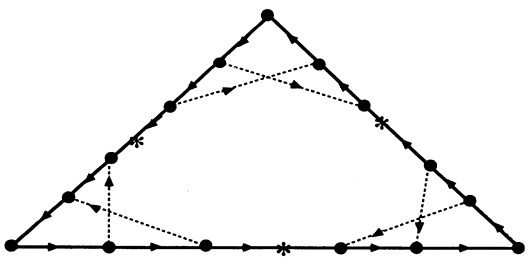

FIG. 4. The graph representing a term obtained by pole decomposition. This graph separates into three disjoint parts when one cuts the three asterisked segments.

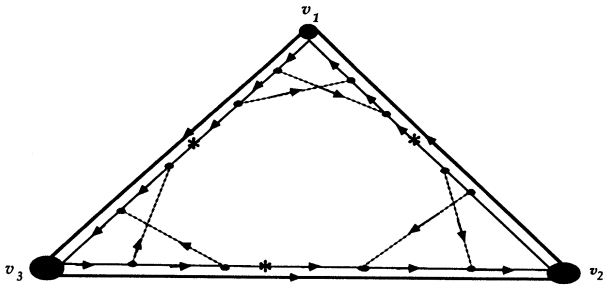

FIG. 5. The Landau diagram associated with the graph of Fig. 4. We distinguish "Landau diagrams" from "graphs": the former are geometric, the latter topological.

where Σ_j is the momentum flowing along segment j of the graph in the direction of the arrow on it, and

$$\sigma_{js}\beta_{js} = \alpha_j \geq 0 \ , \qquad (7c)$$

where the sign σ_{js} is defined below Eq. (4).

(3) Each directed charged-particle line segment s corresponding to a pole denominator $(\Sigma_s^2 - m^2 + i0)$ is represented by a star (asterisk) line segment s, and it represents the vector

$$V_s' = \alpha_s' \Sigma_s \ , \qquad (7d)$$

where Σ_s is the momentum flowing along asterisked line segment s of the graph in the direction shown, and

$$\alpha_s' = \alpha_s - \sum_{j \in J(s)} \beta_{js} \ . \qquad (7e)$$

Here α_s is the Landau parameter α corresponding to the function $f_s = \Sigma_s^2 - m^2 + i0$, and for each side s the set $J(s)$ is the set of indices j that label the pole-residue denominators that are associated with side s of the triangle graph.

(4) Three line segments appear in the Landau diagram that are not images of segments that appear in the graph. They are the three *direct* line segments that directly connect pairs of vertices from the set $\{v_1, v_2, v_3\}$. The vector V_s associated with the direct segment s is

$$V_s = \alpha_s \Sigma_s + \sum_{j \in J(s)} \beta_{js}(\Sigma_j - \Sigma_s) \ . \qquad (7f)$$

It is equal to the sum of the vectors corresponding to the sequence of asterisked and nonasterisked charged-particle line segments that connect the pair of vertices v_i between which the direct line segment s runs.

The p loop equation is represented by the closed loop formed by the three direct line segments V_s specified in (7f). The photon loop equation associated with the photon line carrying momentum k_i is formed by adding to $\alpha_i k_i$ the sum of the vectors corresponding to the charged-particle segments needed to complete a closed loop in the diagram (see Appendix B). Thus the existence of a (nontrivial) solution of the Landau equations is equivalent

to the existence of a (nonpoint) Landau diagram having the specified topological structure, with its line segments equal to the vectors specified in (7). Although Figs. 4 and 5 represent a separable case, the rules described above are general: They cover all cases in which all r_i are nonzero.

For each s we can use in the Landau diagram either V_s' or V_s. We shall henceforth use always V_s, the segment that directly connects a pair of vertices v_i, rather than V_s', and we shall place an asterisk on each of these three direct line segments. These three direct line segments are geometrically more useful than the V_s''s because they display immediately the p loop equations, and also the relative locations of the three external vertices v_i, and because each one has only a single contribution $\alpha_s\Sigma_s$ of well-defined sign and direction, in the limit $k_i \Rightarrow 0$, provided condition (9) (see below) holds.

We specify the way that photon loops pass through Landau diagrams: A photon loop shall pass through the star line s of a *Landau diagram* (i.e., along the direct line segment s) if and only if the corresponding loop in the *graph* passes through the asterisked line s of the *graph*.

The positivity of the photon-line α_i's entails that each directed vector $\alpha_i k_i$ of Fig. 5 points in the positive (energy and/or time) direction (i.e., to the left) if the energy k_i^0 is positive, and in the negative direction (i.e., to the right) if the energy k_i^0 is negative. This fact entails that positive energy is carried by each nonzero (length) photon line segment of Fig. 5 *out of* the vertex that stands on its right-hand end and *into* the vertex that stands on its left-hand end. This result is true independent of the direction in which the arrow points, or of the sign of the energy component k_i^0.

In the general separable case some of the nonasterisked segments may have $\alpha_j = 0$, and hence contract to points. Consequently several photons may emerge from, or enter into, a single vertex of the Landau diagram.

This geometric representation of the "Landau" equations holds only if all $r_i \neq 0$. If one or more $r_i = 0$ then the diagram breaks into parts, as will be seen. We wish to show, by using these geometric conditions and the result (6), that the Ω_i contours can be distorted in such a way as to avoid simultaneously all the singularities except those associated with the three asterisked line poles, one for each of the three sides s of G, and those associated with the various end points $r_i = 0$ and $r_i = 1$. We shall treat the various cases separately.

III. SEPARABLE CASE; ALL $r_i \neq 0$

To prove this result for the separable case, and when all $r_i \neq 0$, let us consider any one of the three disjoint partial diagrams of nonasterisked segments. Let V be the set of vertices of this partial diagram that lie on an end of at least one photon line that is not contracted to a point. Let V_R be any element of V such that every nonzero-length photon line incident upon V_R has its other end lying to the left of V_R. Let V_L be any element of V such that every nonzero-length photon line that is incident upon V_L has its other end lying to the right of V_L. Then the total momentum K carried into either V_R or V_L by all photons incident upon it satisfies $K \neq 0$ and $K^2 \geq 0$. These properties follow from the fact that each photon line of nonzero length incident upon V_R must carry a light-cone-directed momentum energy with positive energy out of V_R, and each photon line of nonzero length incident upon V_L must carry a light-cone-directed momentum energy with positive energy into V_L. However, one cannot satisfy $2pK + K^2 = 0$ with $p \simeq p_1$, p_2, or p_3, and with a small $K \neq 0$ satisfying $K^2 \geq 0$. Consequently the charged-particle line segments of the partial Landau diagram lying on the outer extremities of the two charged particle lines must contract to points, by virtue of (5a): The associated Landau parameter α_i must vanish. Recursive use of this fact entails that *all* of the lines in this partial diagram must contract to a single point.

The existence of zero-length photon lines whose ends do not lie in V does not disturb this argument, provided self-energy parts are excluded.

This result, that each nonasterisked line contracts to a point, means that every entry in every Ω_i loop equation vanishes. Under this condition the lemma expressed by Eq. (6) shows that every Ω_i contour can be distorted away from every Ω_i-dependent singularity. We next show that this result continues to hold when some or all of the r_i vanish.

IV. SEPARABLE CASE; SOME $r_i = 0$

Let us first consider the simple example shown in Fig. 6. The Landau matrix for the diagram of Fig. 6 is shown in Table III. If $r_1 \neq 0 \neq r_2$, then one can multiply the Ω_1^2 row by r_1, multiply the Ω_2^2 row by $r_1 r_2^2$, multiply the last row by r_2, and divide the $d\Omega_2$ column by r_2. This brings the matrix into an equivalent one in which r_1 and r_2 occur only in the combinations $k_1 = r_1\Omega_1$ and $k_2 = r_1 r_2 \Omega_2$: This is the equivalent k form that was previously used for the case $r_1 \neq 0 \neq r_2$.

If $r_1 = 0$ and $r_2 \neq 0$ then one can perform the same transformations involving r_2, and bring the equations to the same form as before, except that the vector associated with the photon line segment 1 is now $\alpha_1\Omega_1$ instead of $\alpha_1 k_1$, and the vector associated with the photon line segment 2 is now $\alpha_2 r_2 \Omega_2$ instead of $\alpha_2 k_2$. The vectors $r_1\Omega_1$ and $r_1 r_2 \Omega_2$ that occur summed with p_1 or p_2 become zero. Thus the situation is geometrically essentially

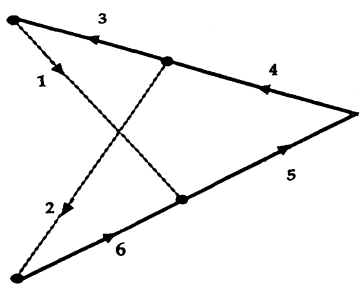

FIG. 6. Part of the diagram of Fig. 5.

TABLE III. The Landau matrix corresponding to the diagram of Fig. 6. The rows corresponding to the conditions $\Omega_j\tilde{\Omega}_j = 1$ have been removed, by using the argument given in Appendix A.

f_j	$d\Omega_1$	$d\Omega_2$
Ω_1^2	Ω_1	0
Ω_2^2	0	Ω_2
$2p_1\Omega_1 + r_1\Omega_1^2$	$p_1 + r_1\Omega_1$	0
$2p_1(\Omega_1 + r_2\Omega_2) + r_1(\Omega_1 + r_2\Omega_2)^2$	$p_1 + r_1\Omega_1 + r_1r_2\Omega_2$	$r_2(p_1 + r_1\Omega_1 + r_1r_2\Omega_2)$
$2p_2(\Omega_1 + r_2\Omega_2) + r_1(\Omega_1 + r_2\Omega_2)^2$	$p_2 + r_1\Omega_1 + r_1r_2\Omega_2$	$r_2(p_1 + r_1\Omega_1 + r_1r_2\Omega_2)$
$2p_2\Omega_2 + r_1r_2\Omega_2^2$	0	$p_2 + r_1r_2\Omega_2$

the same as in the case $r_1 \neq 0 \neq r_2$, though slightly simpler: The small additions k_1 and k_2 to the vectors p_1 and p_2 now drop out. The important point is that the critical denominators $2pK + K^2$ of the earlier argument now take the form $2p\Omega$, with $\Omega^2 \geq 0$ and $\Omega \neq 0$. Such a product cannot vanish. Thus the earlier $r_i \neq 0$ argument goes through virtually unchanged.

If $r_1 \neq 0$ and $r_2 = 0$ then the Ω_1 and Ω_2 loop equations can be considered separately. The earlier $r_i \neq 0$ argument of Sec. III can be applied to the first part alone, and it shows that each line segment on the Ω_1 loop must contract to a point. Next the Ω_2 equation can be considered alone, with each segment along which the Ω_1 loop flows contracted to a point. Then the earlier $r_1 = 0$ arguments can be applied now to this Ω_2 part of the diagram (with r_2 in place of r_1). It shows that each of the segments along which Ω_2 flows also must contract to a point: The corresponding α_j must be zero.

The case $r_1 = r_2 = 0$ is not much different from the case just treated: r_1 enters Table III only in an unimportant way.

The generalization of this argument from the case of Table III to the general separable case is straightforward. Let r_g be the first vanishing element of the ordered set $r_1, r_2, \ldots, r_n$. Then the set of Ω columns of the Landau matrix separates into one part involving only the Ω_i columns for $i < g$, and a second part involving only the Ω_i columns for $i \geq g$. For the first part of this matrix the argument given above for the case with all $r_i \neq 0$ holds, and its entails that every line segment in this part must contract to a point. With all of the rows corresponding to these contracted segments omitted one may apply the $r_1 = 0$ argument (with r_g in place of r_1) to the part $i \geq g$, and proceed iteratively. This argument leads to the conclusion that the only solution to all of the Ω_i loop equations is the trivial one where every entry in every Ω column is zero. Hence the lemma expressed by Eq. (6) ensures that each Ω_i contour can be distorted away from all of its singularities, in the general separable case.

As one moves from the domain where all $r_i > 0$ to the various boundary points where some $r_i = 0$, two kinds of changes can occur. Certain conditions that particular vectors Ω_j be in the upper-half plane with respect to a variable such as $(p_1 + r_1\Omega_1 + r_1r_2\Omega_2)\cdot\Omega_j$ becomes slightly simplified when an r_i becomes zero. Since the different conditions of this kind correspond to vectors p_1, p_2, and p_3 that are well separated, the passage to a point $r_i = 0$ causes no discontinuous change in the set of vectors that satisfy such conditions. The second kind of change is that some contributions to particular $d\Omega_j$'s may suddenly drop out if some r_i vanishes. (See Table III with $r_2 = 0$.) These changes at the boundary points of the region $r_i \geq 0$ do not entail any discontinuity in the distortion of the Ω contours on the boundary. The possibility of using a distortion in Ω space that is everywhere continuous in (r, Ω) follows from the continuousness of the gradients of the functions $f_i(r, \Omega)$, and the fact that at every point in the domain of integration the set of gradients of the set of vanishing f_i form a *convex* set: The Landau equations cannot be satisfied.

V. NONSEPARABLE CASE; ALL $r_i \neq 0$

We consider next the functions represented by graphs such that the cutting of the three asterisked segments does not separate the graph into three disjoint parts. The same result about distortions of Ω_i contours can be obtained also for these functions.

To obtain this result we consider first, as before, the case in which all $r_i \neq 0$. Then we may use the k form of the Landau equations given in (7).

The argument proceeds as before, by making use of the vertices V_R and V_L. No such vertex can join together two pole-residue segments j of nonzero length: It is impossible to satisfy both $2pK_1 + K_1^2 = 0$ and $2pK_2 + K_2^2 = 0$ if $K_1 - K_2 = K$ satisfies $K^2 \geq 0$ and $K \neq 0$, and K_1 and K_2 are small compared to the timelike p. Likewise, neither V_R nor V_L can joint an asterisked segment to a pole-residue segment j with $\alpha_j \neq 0$: One cannot satisfy $2pK + K^2 = (2p + K)K = 0$ if $K^2 \geq 0$ and $K \neq 0$, and K is much smaller than the timelike p. Consequently each of the vertices V_R and V_L must be confined to the set of external vertices v_i:

$$\{V_R, V_L\} \subset \{v_1, v_2, v_3\} \ . \tag{8}$$

In the nonseparable case some of the signs σ_{js} will be negative. Consequently some of the vectors corresponding to pole-residue factors f_j will point in the "reversed" direction, because their β_{js}'s, defined in (7c), are negative. There are also some (sometimes-compensating) reversals of the ways that certain photon loops run. These latter reversals arise because we have used, in the Landau diagrams, the three line segments that directly connect the pairs in $\{v_1, v_2, v_3\}$, rather than the images of the three star lines of the original asterisked graph. For example, the asterisked graph of Fig. 3(c) gives a Landau

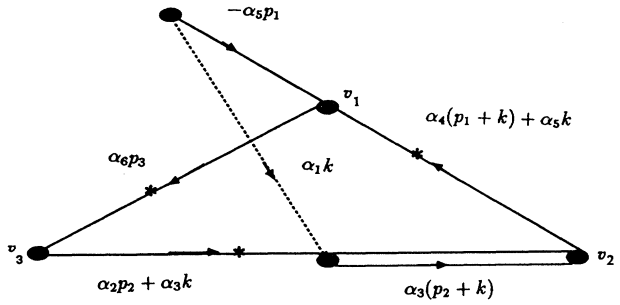

FIG. 7. The Landau diagram corresponding to the asterisked graph of Fig. 3(c). This diagram represents the equations obtained from Table I(c), with f_1 multiplied by r^2, f_3 and f_4 multiplied by r, and $r\Omega$ replaced by k. These changes recover the k form of the equations. The backward orientation of the vector $\alpha_5 p_1$ arises from the negative sign of σ_{51}. However, this vector is oriented against the direction of the photon loop. Consequently all contributions to this photon-loop equation proportional to any p_s have the form $\alpha_j p_s$: The two reversals of the line segment $j=5$ compensate for each other.

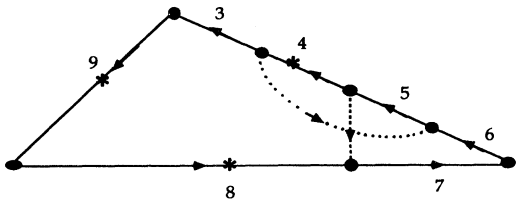

FIG. 8. A graph representing a term in the pole-decomposition expansion. The looping line represents photon 1.

diagram of the form shown in Fig. 7. A second example is the function represented by the graph shown in Fig. 8. The functions f_j and the Landau matrix corresponding to the function represented by the graph in Fig. 8 are shown in Table IV, for $|k_1|>|k_2|>0$. The Landau diagram corresponding to the Landau matrix in Table IV is shown in Fig. 9.

The argument leading to (8) entails more than (8). It shows, in the present case where all $k_i\neq 0$, that each vertex of the diagram that does not lie in $\{v_1,v_2,v_3\}$ and that has at least one nonzero-length photon line segment incident upon it must have at least two nonzero-length photon lines incident upon it: Each such vertex must lie on the right-hand end of at least one such photon line segment, and on the left-hand end of some other such photon line segment. Consequently, every nonzero-length photon line must lie on a "zig-zag" path of photon lines that begins at a vertex in the set $\{v_1,v_2,v_3\}$, moves always to the left, and ends on another vertex in $\{v_1,v_2,v_3\}$: Only in this way can the conditions $K^2\geq 0$ and $K\neq 0$ used in the derivation of (8) be overcome, if all k_i are different from zero.

Consider, then, an example with vertices labeled as in Fig. 10. Suppose $V_l=v_3$ and $V_R=v_1$ are the unique V_L and V_R. Then some sequence of photon lines of nonzero length must join together to give a zig-zag path from v_1 to v_3. Three examples are shown in Fig. 11.

To analyze such diagrams we assume temporarily that for all pertinent solutions of the Landau equations

$$|\alpha_j|\leq|\alpha_s|B \quad \text{for } j\in J(s)\ , \tag{9}$$

where B is some fixed finite number. That is, we exclude temporarily the case where some α_j becomes unbounded, with the α_s bounded. Then as one lets the δ' in (3) tend to zero the vector V_s defined in (7f) and, for $j\in J(s)$, the vectors V_j defined in (7b) all become increasingly parallel to p_s.

Consider then a sequence of bounds δ'_t, $t=1,2,\ldots$, that tend to zero, and a corresponding sequence of solutions S_t to the Landau equations in which (1) $k_i\neq 0$, $i=1,\ldots,n$, (2) $|k_i|\leq\delta'_t/n$, $i=1,\ldots,n$, (3) some $\alpha_i k_i\neq 0$, and (4) condition (9) holds.

If $q^t=(q_1^t,q_2^t,q_3^t)$ is the vector $q=(q_1,q_2,q_3)$ specified by S_t, then any accumulation point $\bar{q}$ of the set $\{q^t\}$ must be specified by a limiting diagram in which every charged-particle segment is parallel to one of the vectors p_s, $s\in\{1,2,3\}$, and in which some zig-zag path of light-cone vectors runs leftward from a vertex V_R of $\{v_1,v_2,v_3\}$ to a vertex V_L of $\{v_1,v_2,v_3\}$, but carries zero momentum energy. The limit point $\bar{q}$ must therefore lie on the Landau triangle diagram singularity surface $\varphi(q)=0$. However, the presence of the zig-zag photon line connecting two of the three vertices v_i imposes an extra condition, which defines a codimension-one submanifold of $\varphi(q)=0$. These submanifolds are finite in number (for

TABLE IV. The Landau matrix for the function represented by the graph in Fig. 8, for $|k_1|>|k_2|>0$. The sign of σ_{j1} is minus for $j=3$ and 6, and otherwise plus.

f_j	dk_1	dk_2	dp
$f_1=k_1^2$	k_1	0	0
$f_2=k_2^2$	0	k_2	0
$f_3=2p_1k_1+k_1^2$	p_1+k_1	0	k_1
$f_4=(p_1+k_1)^2-m^2$	p_1+k_1	0	p_1+k_1
$f_5=2p_1k_2+2k_1k_2+k_2^2$	k_2	$p_1+k_1+k_2$	k_2
$f_6=2p_1(k_1-k_2)+k_1^2-k_2^2$	p_1+k_1	$-(p_1+k_2)$	k_1-k_2
$f_7=2p_2k_2+k_2^2$	0	p_2+k_2	k_2
$f_8=p_2^2-m^2$	0	0	p_2
$f_9=p_3^2-m^2$	0	0	p_3

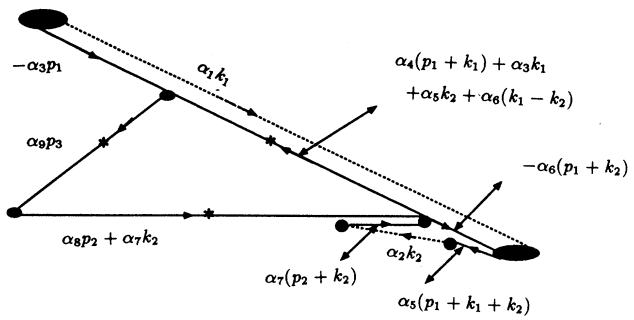

FIG. 9. The "Landau diagram" that represents the Landau equations associated with the Landau matrix shown in Table IV. This diagram is not a true Landau diagram, because, for example, the vector $\alpha_i k_i$ cannot be a light-cone vector. Moreover, condition (8) is not satisfied. Were it not for the non-negativity condition on α_3, one could satisfy the Landau equations with $\alpha_3 = -\alpha_4$, and $\alpha_1 = \alpha_2 = \alpha_5 = \alpha_6 = \alpha_7 = 0$.

any fixed graph g), and hence are nondense in the interior of $\varphi = 0$. If a point $q \in \{\varphi = 0\}$ lies at a nonzero distance from each of these submanifolds then no solution of the kind specified above can occur, and hence for some sufficiently small neighborhood N of q, and for some sufficiently small δ', any solution to the Landau equations for $q \in N$ satisfying $0 < |k_i| \leq \delta'/n$ for all i, and conditions (2) and (5), can have only zero-length photon lines: i.e., for all photon lines i,

$$\alpha_i k_i = 0 \ . \tag{10}$$

We are interested here in the singularity structure at a general point on $\varphi = 0$, rather than at special points where other singularity surfaces are relevant. Hence we may restrict our attention to a neighborhood N in $\varphi = 0$ where (10) holds.

Condition (10) says that every photon line segment i must have zero length. This condition entails the stronger result that every segment on every photon loop i in the Landau diagram must contract to a point.

To obtain this stronger result consider *in order* the loop equations corresponding to the sequence of variables

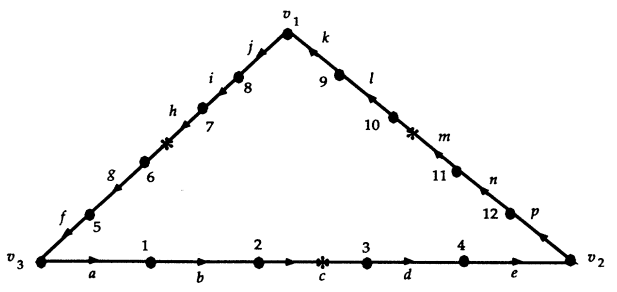

FIG. 10. A triangle graph with photon vertices labeled by numbers, and charged-particle line segments labeled by letters. The segments h, c, and n are asterisked segments associated with the pole-decomposition formula (1′). The photon lines have been suppressed.

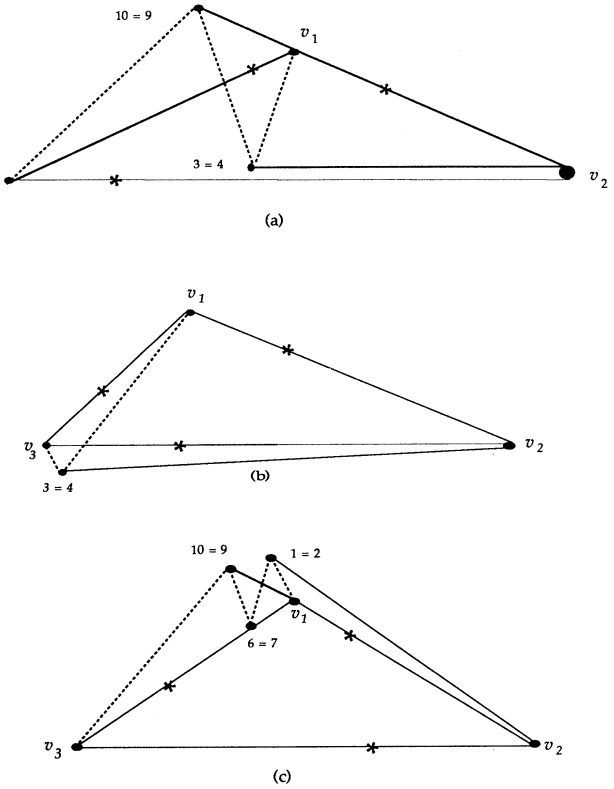

FIG. 11. Three diagrams with zig-zag paths of photons connecting v_1 to v_3.

$k_1, \ldots, k_n$, as defined in the formula (1). Consider first, then, the closed loop 1 in the Landau diagram. For each charged-particle segment on this loop the k_l with smallest l that flows along this loop 1 is k_1 itself. Consequently the orientations of all of the segments along this loop are unambiguously determined: For each $s \in \{1, 2, 3\}$ every contribution to the loop 1 that arises from a charged-particle segment on side s *adds* to the loop equation a vector that is very close to a non-negative multiple of p_s, just as in Figs. 7 and 9. Use can be made here of the facts [8–11] that the triple of four-vectors (v_1, v_2, v_3) specified by the three external vertices v_i constitute a normal to the Landau surface [in $q = (q_1, q_2, q_3)$ space] associated with the diagram, and that this surface can be tangent to the triangle diagram Landau surface $\varphi(q) = 0$ at a point q only if the directions of the three vectors V_s are the same as they are for the simple Landau diagram that corresponds to Table I. Because we are staying away from exceptional points of lower dimension the three vectors V_s must be parallel to the three vectors p_s. Alternatively, one can use the condition (9), and take δ' sufficiently small, in order to deduce that V_s is approximately equal to $\alpha_s p_s$.

Each photon loop passes along at most *two* sides s of the triangle. Hence, on any single photon loop in the Landau diagram, each charged-particle segment points approximately in the direction of one or the other of at most *two* of the three vectors p_s. (See Figs. 7 and 9.) Hence the contraction to a point, demanded by (10), of

the remaining segment of the loop (namely, $\alpha_1 k_1$) forces every segment on loop 1 to contract to a point.

Consider next the loop 2. All segments along with k_1 runs have now been contracted out. Thus the k_l with the smallest value of l that flows along the surviving part of loop 2 is k_2 itself. Hence each segment on this loop also must contract to a point, by the same argument that was just used for loop 1. Proceeding step by step, one finds that every segment on every photon loop must contract to a point.

In this nonseparable case with all $r_i \neq 0$ at least one photon line must pass along an asterisked line. Hence at least one of the three asterisked lines of the Landau diagram must also contract to a point. But then the other two sides of the triangle (v_1, v_2, v_3) must also contract to points, since, in accordance with the conditions imposed below Eq. (2), the three sides of the triangle connecting the three vertices v_i are nonparallel. But then every segment of the Landau diagram is forced to a point, and thus there is no solution of the Landau equations, in this nonseparable case with all $r_i \neq 0$.

This conclusion was derived under the assumption (9). However, that assumption is not necessary. Suppose we normalized the solutions by requiring that $\max |v_i - v_j| = 1$, and drop (9). Then the direction of V_s is not constrained, but its Euclidean length is.

Consider, under these conditions, the sequence of loops i. A first part of loop 1 consists of either the zero, one, or two vectors V_s that are included on the loop. Their directions are indeterminate, but their magnitudes are at most unity. In fact the magnitude of the sum of these segments is at most unity.

A second part of this closed loop is the segment corresponding to the photon 1 itself. The length of this segment is limited by the fact that any nonzero-length photon line segment must lie on a zig-zag path that runs between two of the vertices v_i, and is composed of leftward-pointing light-cone vectors. Since the Euclidean distance between the end points of this zig-zag path is bounded by unity, the individual segments along this path are likewise bounded. Thus these first two parts of loop 1 are bounded.

The third and final part of loop 1 is the sum of the contribution of the segments j associated with the pole-residue denominators f_j. All of these contributions to the loop are essentially of the form $\alpha_j p_s$, with all the α_j's positive, and s ranging over either *one or two* of its three possible values. (See Figs. 7 and 9.) We can impose the condition that at the points $q \in \{\varphi = 0\}$ under consideration the three vectors p_s are *far* from parallel. In this case the bound on the first two parts of the closed loop 1 imposes a comparable bound on the third part, and, in particular, a bound on the sum of the α_j corresponding to those segments j that lie on loop 1.

We then turn to loop 2. Bounds are established as before for all parts of loop 2 that are not pole-residue segments j, and also for all pole-residue segments j that lie on loop 1. Since the contributions from the pole-residue segments j that lie on loop 2 but not loop 1 have the form $\alpha_j p_s$, with $\alpha_j \geq 0$, and with s ranging over at most two of the three possible values, we can now establish upper bounds on the sum of these new α_j's. Proceeding in this way we establish bounds on all of the α_j's associated with all the pole-residue denominators f_j. Then for a sufficiently small δ' we can ensure that, for each value of s, the contribution to V_s, specified by (7f), that arises from the photon momenta k_i is small compared to this vector V_s itself. This is the result that in the earlier argument was obtained from (9), which we therefore no longer need.

VI. NONSEPARABLE CASE; SOME $r_i = 0$

The results for the $k_i \neq 0$ case carry over to the general situation, provided the (r, Ω) variables are retained. The argument for the case where some $r_i = 0$ proceeds much as in the case of separable diagrams. Let r_g be the first vanishing member of the ordered sequence $r_1, r_2, ..., r_n$. Then the Landau matrix separates into two parts. The first consists of the $d\Omega_i$ columns for $i < g$, plus the dp column; the second consists of the $d\Omega_i$ columns for $i \geq g$. By multiplying and dividing various rows and columns of the Landau matrix by appropriate nonzero factors r_i $(i < g)$, one can convert the $i < g$ part to the k form, with all k_j for $j \geq g$ set to zero. The $r_i \neq 0$ argument can then be applied to these $i < g$ Landau equations: They imply the vanishing of the α_j's corresponding to all segments j of the Landau diagram along which run the photon loops i with $i < g$.

The remaining columns, which give the $i \geq g$ part of the Landau equations, can be separated into *sectors*, where each sector begins with a column $d\Omega_i$ such that $r_i = 0$, and is followed by the set of columns $d\Omega_{i+1}, ..., d\Omega_{i+h}$ such that $r_{i+1}, ..., r_{i+h}$ are all nonzero. The latter r's can be changed to unity without altering the content of the Landau equations. We shall do this, purely for notational convenience.

The rows corresponding to the three pole denominators do not contribute to the $i \geq g$ equations because

$$\frac{1}{2}\frac{\partial}{\partial \Omega_g}[(p + r_1 \cdots r_j \Omega_j + \cdots)^2 - m^2] = 0 \quad \text{for } j \geq g \ ,$$

due to $r_g = 0$.

One proceeds step by step, starting with the $i < g$ part, then considering the various individual sectors, in order of increasing values of i. The Landau equations for each one of the individual sectors can be expressed by a Landau diagram constructed in accordance with the rules (7), with, however, the following changes. (1) The three vectors V_s corresponding to the three direct line segments s are set to zero; (2) all the segments of the Landau diagrams that occur at earlier stages of the step-by-step process are contracted to points; and (3) the photon propagator contribution $\alpha_i k_i$ to each $d\Omega_i$ column that belongs to the sector in question is replaced by $\alpha_i \Omega_i$.

The Landau diagram corresponding to a sector S has a "spider" form: It consists of a single central vertex v, which represents the three coincident vertices v_i, plus a web of segments sprouting out from v. All segments of the Landau diagrams corresponding to the previously considered sectors are contracted to the single point v, to-

gether with all of the segments that constitute the part $i < g$. All charged-particle segments of the Landau diagram along which run *none* of the photon loops that constitute S are also contracted to points.

The Landau diagram that corresponds to any individual sector S can be shown to contract to a point by using the arguments developed earlier: The argument involving V_R and V_L shows that no photon line of nonzero length can occur in the spider diagram, and then the step-by-step consideration of the photon loops i, in the order of increasing i, shows that each of these loops must contract in turn to a point.

We thus conclude that for every j such that the Landau matrix element

$$L_{ij} \equiv \tfrac{1}{2}\partial f_j/\partial\Omega_i \ ,$$

is nonzero for some i, $\alpha_j = 0$. But then the lemma represented by Eq. (6) entails that one can distort the Ω_i contours in such a way as to move simultaneously into the upper-half plane of each of the residue-factor denominators f_j and each of the photon-propagator denominators $(\Omega_j)^2$. The only remaining singularities are the end-point singularities at $r_i = 0$ and $r_i = 1$, and the three Feynman denominators associated with the three asterisked lines of the asterisk graph g: For every other singularity surface $f_j = 0$ there is some Ω_i such that $L_{ij} \neq 0$ for the corresponding j and i. The consequences of the three asterisked line singularities in conjunction with the end-point singularities in the radial variables r_i are dealt with in papers I and III.

ACKNOWLEDGMENTS

This work was supported by the Director, Office of Energy Research, Office of High Energy and Nuclear Physics, Division of High Energy Physics of the U.S. Department of Energy under Contract No. DE-AC03-76SF00098, and by the Japanese Ministry of Education, Science and Culture under a Grant-in-Aid for Scientific Research (International Scientific Research Program 03044078).

APPENDIX A: PROOF OF THE TRIVIALITY OF THE CONTRIBUTION FROM THE FACTOR $\delta(\Omega_J\tilde{\Omega}_J - 1)$ TO THE LANDAU LOOP EQUATIONS

In discussing the singularities of the meromorphic parts in Sec. VIII, we made full use of the fact that the row in the Landau matrix corresponding to $\Omega_j\tilde{\Omega}_j - 1$ reduces to zero under the closed loop conditions for the Ω_j, r_j, and the r_{j+1} columns. We give here a proof of this fact.

In view of the definition of the integral, the functions f_i other than the various $\Omega_j^2, \Omega_j\tilde{\Omega}_j - 1$ and r_j have the form (A1) or (A2), where ϵ_m and ϵ_t' are each either 0, +1, or −1;

$$f_i = \left(p_l + \sum \epsilon_m r_1 \cdots r_m \Omega_m\right)^2 - m^2 \ , \tag{A1}$$

$$\begin{aligned} f_i = {} & 2\left(p_l + \sum \epsilon_m r_1 \cdots r_m \Omega_m\right) \\ & \times \left(\Omega_s + \sum \epsilon_t' r_{s+1} \cdots r_t \Omega_t\right) \\ & + r_1 \cdots r_s \left(\Omega_s + \sum \epsilon_t' r_{s+1} \cdots r_t \Omega_t\right)^2 \ . \end{aligned} \tag{A2}$$

Let H_j denote the first-order differential operator given by $\Omega_j \frac{\partial}{\partial\Omega_j} - r_j \frac{\partial}{\partial r_j} + r_{j+1} \frac{\partial}{\partial r_{j+1}}$. Then the following equations hold:

$$H_j \left(p_l + \sum \epsilon_m r_1 \cdots r_m \Omega_m\right) = 0 \ \text{ for any } j \text{ and } l \ . \tag{A3}$$

$$H_j \left(\Omega_s + \sum \epsilon_t' r_{s+1} \cdots r_t \Omega_t\right) = \begin{cases} \Omega_s + \sum \epsilon_t' r_{s+1} \cdots r_t \Omega_t & \text{if } j = s \ , \\ 0 \ \text{ if } j \neq s \ , \end{cases} \tag{A4}$$

$$H_j \left[r_1 \cdots r_s \left(\Omega_s + \sum \epsilon_t' r_{s+1} \cdots r_t \Omega_t\right)^2\right] = \begin{cases} r_1 \cdots r_s \left(\Omega_s + \sum \epsilon_t' r_{s+1} \cdots r_t \Omega_t\right)^2 & \text{if } j = s \ , \\ 0 \ \text{ if } j \neq s \ . \end{cases} \tag{A5}$$

Hence H_j annihilates each f_i of the form (A1) and each f_i of the form (A2) with $s \neq j$, and it reproduces each f_i of the form (B2) with $s = j$.

Since the Ω_j column, etc. in the Landau matrix is given by $\partial f_i/\partial\Omega_j$, etc., this property of the operator H_j entails, under the Ω_j, r_j, and r_{j+1} closed-loop conditions, that

$$
\begin{aligned}
0 &= \Omega_j \left(\sum_i \alpha_i \frac{\partial f_i}{\partial \Omega_j} \right) - r_j \left(\sum_i \alpha_i \frac{\partial f_i}{\partial r_j} \right) \\
&\quad + r_{j+1} \left(\sum_i \alpha_i \frac{\partial f_i}{\partial r_{j+1}} \right) \\
&= \sum_i \alpha_i H_j f_i \\
&= \sum_{i \in I(j)} \alpha_i f_i + 2a_j \Omega_j^2 + 2\beta_j \Omega_j \tilde{\Omega}_j - \gamma_j r_j + \gamma_{j+1} r_{j+1} \ ,
\end{aligned}
$$

where $I(j)$ denotes the set of indices i such that f_i is of the form (A2) with $s = j$, and a_j, β_j, and γ_j denote the Landau parameters associated with Ω_j^2, $\Omega_j \tilde{\Omega}_j - 1$, and r_j, respectively. It follows from (5a) that all terms except for $\beta_j \Omega_j \tilde{\Omega}_j = \beta_j$ on the right-hand side of (A6) vanish. This entails the required fact, namely, that the row corresponding to $\Omega_j \tilde{\Omega}_j - 1$ must have coefficient $\beta_j = 0$ and hence give no net contribution to the Landau loop equations.

APPENDIX B: THE LANDAU DIAGRAM CORRESPONDING TO A TERM IN THE POLE-DECOMPOSITION EXPANSION

To confirm the geometric representation of the Landau equations described in connection with Eq. (7), recall first that the pole-residue denominators corresponding to nonasterisked charged lines are

$$
f_j = \sigma_{js} (\Sigma_j^2 - \Sigma_s^2) + i0 \ , \tag{B1}
$$

where the sign σ_{js} is defined below Eq. (4). For each side $s \in \{1, 2, 3\}$ one may verify immediately that the contribution from the side s of the triangle of *direct* lines V_s is just the contribution to the p loop equation arising from the charged-particle line segments that lie on side s of the original graph.

For the photon loop l there is first a contribution $\alpha_k k_l$, and then the contributions corresponding to charge-particle line segments along which the loop flows. There are contributions of this latter kind only from segments corresponding to those (one or two) sides s of the triangle along which the loop runs, and we can consider separately the contributions from each of those sides s.

There are three cases.

Case (1). The photon loop l in the Feynman graph runs along the segment $j \in J(s)$ but does *not* run along the asterisked segment lying on side s. In this case the contribution to the l loop equation proportional to α_j is

$$
\begin{aligned}
\alpha_j \frac{1}{2} \frac{\partial f_j}{\partial k_l} &= \sigma_{js} \alpha_j \frac{1}{2} \frac{\partial}{\partial k_l} (\Sigma_j^2 - \Sigma_s^2) \\
&= \beta_{js} \Sigma_j \ .
\end{aligned} \tag{B2}
$$

Case (2a). The loop l of the Feynman graph flows along the asterisked segment of side s, but does *not* flow along the nonasterisked segment j lying on side s. Thus the contribution to the l loop equation proportional to α_j is

$$
\begin{aligned}
\alpha_j \frac{1}{2} \frac{\partial f_i}{\partial k_l} &= \sigma_{js} \alpha_j \frac{1}{2} \frac{\partial}{\partial k_l} (\Sigma_j^2 - \Sigma_s^2) \\
&= \beta_{js} (-\Sigma_s) \ .
\end{aligned} \tag{B3}
$$

Case (2b). The loop l of the Feynman graph flows along the asterisked segment of side s of the graph and also along the nonasterisked segment $j \in J(s)$. Then the contribution to the l loop equation proportional to α_j is

$$
\begin{aligned}
\alpha_j \frac{1}{2} \frac{\partial f_j}{\partial k_l} &= \beta_{js} \alpha_j \frac{1}{2} \frac{\partial}{\partial k_l} (\Sigma_j^2 - \Sigma_s^2) \\
&= \beta_{js} (\Sigma_j - \Sigma_s) \ .
\end{aligned} \tag{B4}
$$

Notice that, according to (B2), (B3), and (B4), there is, for each $j \in J(s)$, a contribution $\beta_{js} \Sigma_j$ to the photon loop equation l if and only if the loop l in the graph passes along the segment j. There is also, for each $j \in J(S)$, a contribution $-\beta_{js} \Sigma_s$ if and only if this loop passes along the asterisked line s in the graph. There is also a contribution $\alpha_s \Sigma_s$ if and only if this loop passes along the star line s of the graph. These results are summarized by the equations (7).

[1] T. Kawai and H. P. Stapp, preceding paper, Phys. Rev. D **52**, 2484 (1995); See also H. P. Stapp, *ibid.* **28**, 1386 (1983).

[2] H. P. Stapp, in *Structural Analysis of Collision Amplitudes*, edited by R. Balian and D. Iagolnitzer (North-Holland, New York, 1976), p. 200 (Pham's Theorem).

[3] L. D. Landau, in "Proceedings of the Kiev Conference on High-Energy Physics, 1959" (unpublished); Nucl. Phys. **13**, 181 (1959); N. Nakanishi, Prog. Theor. Phys. **22**, 128 (1959).

[4] R. J. Eden, P. V. Landshoff, D. I. Olive, and J. C. Polkinghorne, *The Analytic S-Matrix* (Cambridge University Press, Cambridge, 1966), p. 57.

[5] T. Kawai and H. P. Stapp, in *Algebraic Analysis*, edited by M. Kashiwara and T. Kawai (Academic, New York, 1988), Vol. 1.

[6] T. Kawai and H. P. Stapp, Publ. RIMS Kyoto Univ. Suppl. 12, 155 (1977), Theorem 2.1.1.

[7] J. Coster and H. P. Stapp, J. Math. Phys. **11**, 2743 (1970) (see p. 2758).

[8] C. Chandler and H. P. Stapp, J. Math. Phys. **10**, 826 (1969).

[9] D. Iagolnitzer and H. P. Stapp, Commun. Math. Phys. **14**, 15 (1969).

[10] H. P. Stapp, in *Structural Analysis of Collision Amplitudes*, edited by R. Balian and D. Iagolnitzer (North-Holland, New York, 1976).

[11] D. Iagolnitzer, *The S-Matrix* (North-Holland, Amsterdam, 1978); Commun. Math. Phys. **41**, 39 (1975); **63**, 49 (1978).